CHEMISTRY
A EUROPEAN JOURNAL

FULL PAPER

DOI: 10.1002/chem.201302264

Organocatalyzed Aldol Reaction Between Pyridine-2-carbaldehydes and α-Ketoacids: A Straightforward Route towards Indolizidines and Isotetronic Acids

Virginie Liautard, Damien Jardel, Clotilde Davies, Muriel Berlande, Thierry Buffeteau, Dominique Cavagnat, Frédéric Robert,* Jean-Marc Vincent,* and Yannick Landais*[a]

Abstract: Enantioselective aldol reactions between substituted pyridine carbaldehydes and α-ketoacids were shown to provide isotetronic acids or their corresponding pyridinium salts, depending on the nature of the substituents on the pyridine ring. The pyridinium salts were generated through nucleophilic attack of the pyridine nitrogen atom onto the reactive keto functional group. Moderate-to-good yields of both compounds were typically obtained and high levels of enantioselectivity were observed by using benzimidazole pyrrolidine **I** as a catalyst. Hydrogenation of the resulting pyridinium salts led to new indolizidines with high *ee* values and diastereocontrol. X-ray diffraction studies allowed the determination of the relative configuration of the products. Finally, DFT calculations were performed to rationalize the divergent pathway as a function of the pyridine substituents.

Keywords: aldol reaction · enantioselectivity · heterocycles · indolizidines · organocatalysis

Introduction

The organocatalyzed aldol reaction has been at the onset of the "renaissance" of aminocatalysis[1] and it is still the subject of intense research activity, with the development of more-efficient catalysts and their utilization in the total synthesis of natural products.[2] In this context, some years ago, we reported the development of a readily available benzimidazole pyrrolidine catalyst (**I**, "BIP") that was derived from L-proline and exhibited remarkable reactivity in various reactions, including aldol reactions.[3] Whereas most catalysts require the use of an excess of one of the reagents (usually the ketone donor), catalyst **I** has been shown to catalyze aldol processes by using an equimolar amount of the ketone and aldehyde partners. Amongst the various aldol processes that have been catalyzed by compound **I**, a straightforward synthesis of isotetronic acids **3** from α-ketoacids (e.g. **2**) and aromatic or aliphatic aldehydes was developed, thus leading to the desired five-membered rings in high yields and with high enantioselectivities.[4] This work complemented previous approaches to isotetronic acids by using chiral auxiliaries, organometallic catalysis, and proline-catalyzed pyruvate homo-aldol reactions and represents one of the few examples of organocatalyzed asymmetric aldol reactions that exploit 1,2-dicarbonyl compounds as pronucleophiles.[5]

Naturally occurring isotetronic acids exhibit relevant biological properties,[6] including inhibitory activity of aldose reductase[6a] and antitumor activity against various carcinomas.[6b] These simple motifs are also found as key fragments in more-complex targets, such as erythronolide A.[6d] During the course of our studies on organocatalyzed aldol reactions, we made some unexpected observations in the aldol reactions between pyridine-2-carbaldehydes **1** and various α-ketoacids **2** (Scheme 1). The long-standing interest of this class of compounds and recent efforts towards their synthesis[7] prompted us to provide a full report on these unexpected results herein.

[a] Dr. V. Liautard, D. Jardel, C. Davies, M. Berlande, Dr. T. Buffeteau, Dr. D. Cavagnat, Dr. F. Robert, Dr. J.-M. Vincent, Prof. Dr. Y. Landais
Université de Bordeaux
Institut des Sciences Moléculaires, UMR-CNRS 5255
351, cours de la liberation, 33405 Talence Cedex (France)
Fax: (+33) 540006286
E-mail: f.robert@ism.u-bordeaux1.fr
jm.vincent@ism.u-bordeaux1.fr
y.landais@ism.u-bordeaux1.fr

Supporting information for this article, including the experimental details, characterization data of the products, spectra of new compounds, computational details, energy values, and Cartesian coordinates of the structures discussed in the text, is available on the WWW under http://dx.doi.org/10.1002/chem.201302264.

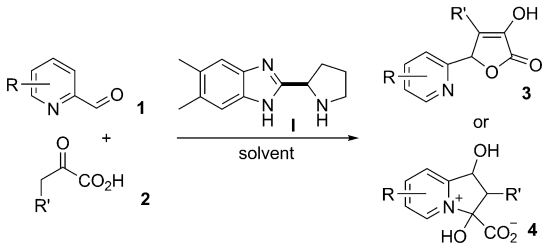

Scheme 1. Aldol reactions between pyridine carbaldehydes **1** and α-ketoacids **2** catalyzed by compound **I**.

Depending on the nature of the substituents on the pyridine skeleton, the reactions between compounds **1** and pyruvic-acid derivatives **2** were shown to effectively provide the desired isotetronic acids **3** or, more surprisingly, their corresponding pyridinium salts **4** (Scheme 1). To the best of our knowledge, this transformation has never been reported before. Interestingly, complete hydrogenation of the pyridinium salts **4** eventually led to the corresponding non-natural indolizidines[8] in good yields and with high enantiocontrol in only two steps from commercially available precursors. This reaction likely proceeded through the stereoselective addition of an enamine that was formed from the α-ketoacid **2** and catalyst **I** onto the aldehyde functional group of pyridine **1**; subsequent lactonization provided compound **3**.[4] Alternatively, the resulting aldol product may evolve through the attack of the pyridine nitrogen atom onto the electrophilic α-keto group to provide compound **4**. Herein, we describe the development of this unusual organocatalyzed aldol reaction, which results in the formation of new C–C and C–N bonds and the generation of up to five stereogenic centers in only two steps. We discuss the scope and limitations of our method, provide a rationalization of the effects that favor the formation of compound **4** over compound **3**, supported by DFT calculations, and describe some useful transformations of aldol products **4**. Finally, the configurations of some pyridinium salts, both in the solid state and in solution, are discussed based on IR and vibrational circular dichroism (VCD) studies, associated with theoretical calculations.

Results and Discussion

Preliminary studies were performed by reacting pyridine carbaldehyde **1a** with α-ketobutyric acid **2a** in the presence of 10 mol% of catalyst **I** (Table 1; an optimized synthesis of catalyst **I** is given in the Supporting Information). In contrast with previous results, the corresponding isotetronic acid **3a** was not observed with this particular aldehyde; instead a pyridinium salt **4a** was isolated in various amounts, depending on the reaction conditions and on the isolation process. The enantioselectivity of compound **4a** could not be obtained through chiral HPLC and, thus, was evaluated by measuring the optical rotation of the sample in various solvents. The optical rotation of enantiomerically pure pyridinium **4a** was estimated based on the observation that a sample of compound **4a** in THF (Table 1, entry 9) led to indolizidine **6a**, after reduction under PtO_2 catalysis[9] and benzylation of acid **5a**, with an *ee* value of >99% (Scheme 2). In all cases, after evaporation of the solvent at room temperature and column chromatography on silica gel (CH_2Cl_2/MeOH), compound **4a** was obtained as a single isomer and its structure was unambiguously determined through X-ray diffraction studies (see below; Scheme 2). The relative and absolute configurations of zwitterion **5a** were also determined by X-ray diffraction studies. As shown in Table 1, the best results were obtained in THF, CH_2Cl_2, Et_2O, and MeOH, with better optical purity in the former solvent. Interestingly, pyridinium **4a** was found to precipitate out of THF, thereby allowing its isolation by simple filtration. The reaction also proceeded in water, although it provided compound **4a** in a mixture of unidentified products, whereas, in 1,4-dioxane, compound **4a** was almost racemic. No trace of compound **4a** could be detected when the reaction was performed without solvent (Table 1, entry 1). Small amounts of compound **4a** were formed in DMF, but evaporation of the solvent essentially led to degradation (Table 1, entry 2). When the reaction was performed in the absence of a catalyst or with L-proline, no trace amounts of isotetronic acids or pyridinium salts could be detected. We previously showed that under acidic conditions, proline proved to be poorly reactive.[3a] Finally, attempts to extend this method to α-ketoesters instead of their corresponding acids were unsuccessful.

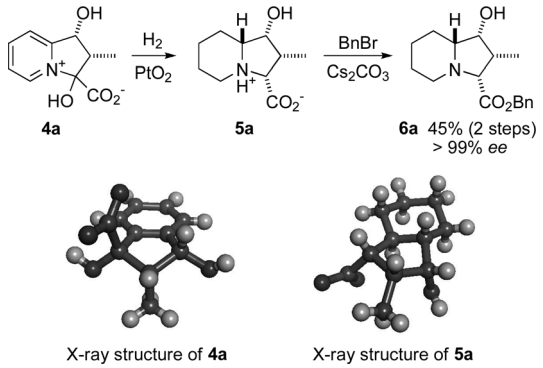

Scheme 2. Reduction of compound **4a** and X-ray structures of compounds **4a** and **5a**.

Table 1. Aldol reaction between pyridine **1a** and α-ketobutyric acid **2a**.

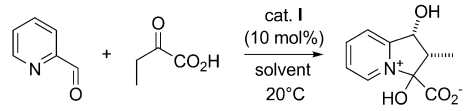

1a **2a** **4a**

Entry	Solvent	Yield of **4a** [%][a]	Optical rotation of **4a** (*c*)[b]	Estimated *ee* of **4a** [%][c]
1	neat	0	–	–
2	toluene	57	−11.3 (0.52, MeOH)	33
3	Et_2O	74	−26.9 (0.505, MeOH)	78
4	DMF	0	–	–
5	water	34	−26.9 (0.52, MeOH)	62
6	CH_2Cl_2	70	−27.3 (0.52, MeOH)	80
7	1,4-dioxane	60	0.9 (0.52, MeOH)	−3
8	MeOH	78	−28.2 (0.52, MeOH)	82
9	THF	75	−34.3 (0.56, MeOH)	>99

[a] Yield of isolated compound **4a** after column chromatography (CH_2Cl_2/MeOH). [b] Reaction was performed at 25 °C. [c] Enantiomeric excess of compound **4a**: $ee = [\alpha]_{D\,exp}/[\alpha]_{D\,pure\,\mathbf{4a}\times 100}$, by using $[\alpha]_{D\,pure\,\mathbf{4a}} = -34.3$ ($c = 0.51$, MeOH) (see text).

With these results in hand, we varied the nature of the substituents on the pyridine carbaldehyde by using compound **2a** as the enamine precursor. The results shown in Table 2 indicate that the nature of the substituents on pyridine **1** has a strong influence on the outcome of the reaction. The presence of hydrogen, methyl, or fluorine groups at the C5 position (**1a**, **1b**, and **1d**; Table 2, entries 1, 2, and 4) exclusively afforded the corresponding pyridinium compounds (**4a**, **4b**, and **4d**, respectively), in generally good yields as a single diastereomer for both the enantiomeric and racemic series. Changing the position of the Me substituent (to the C2 position) as in compound **1c** also led to pyridinium **4c** (Table 2, entry 3). In contrast, other electron-withdrawing substituents (Table 2, entry 5–7) and also electron-donating substituents (Table 2, entries 8 and 9) exclusively led to their corresponding isotetronic acids in good yields and high enantioselectivities (measured or estimated by chiral HPLC). As above, the enantiomeric excesses for pyridiniums **4a**–**4d** could not be directly determined by HPLC analysis and, thus, were estimated after further functionalization (see below). Similar to compound **4a**, the relative configurations of compounds **4b** and **4c** were determined by X-ray diffraction (see the Supporting Information), after further elaboration of the pyridine ring (see below).

Table 2. Aldol reactions between pyridines **1a**–**1k** and **2a**.

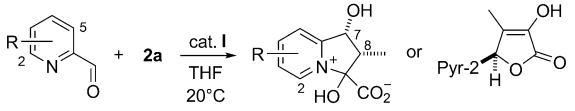

1a–k **4a–d** **3e–k**

Entry	1	R	3	Yield of 3 [%][a,b]	*ee* of 3 [%][c]	4	Yield of 4 [%][a,b]
1	**1a**	H	–	–	–	**4a**	75 (82)
2	**1b**	5-Me	–	–	–	**4b**	73 (80)
3	**1c**	2-Me	–	–	–	**4c**	77 (41)
4	**1d**	5-F	–	–	–	**4d**	29 (41)
5	**1e**	2-Br	**3e**	73 (52)	93	–	–
6	**1f**	2-CHO	**3f**	42 (20)	n.d.	–	–
7	**1g**	2-*p*-CNPh	**3g**	69 (72)	75	–	–
8	**1h**	2-OMe	**3h**	84 (82)	89	–	–
9	**1i**	2-pyrrolidinyl	**3i**	55 (14)	82	–	–
10	**1j**	3-Br	**3j**	75 (90)	98	–	–
11	**1k**	3-CN	**3k**	63 (50)	90	–	–

[a] Yield of isolated product after column chromatography (see the Supporting Information). [b] Yield of isolated compound as a racemate (reaction performed with (+/-)-**I**) is given in parentheses. [c] Enantiomeric excesses were measured by chiral HPLC (Chiralpak AD-H and IA columns). n.d. = not determined.

Having established the reactivity of α-ketoacid **2a** in the presence of various pyridine carbaldehydes, we studied the effects of the nature of α-ketoacid substituents on the formation of pyridinium salts **4**. The reactions of pyridine carbaldehydes **1a** and **1b** with α-ketoacids **2b**–**2d** led to salts **4e**–**4h** in moderate-to-good yields with high levels of diastereocontrol (except for compounds **4f** and **4h**; Scheme 3).[10] Moderate yields resulted from the formation of unidentified by-products, which were discarded upon crystallization. To the best of our knowledge, the reaction that provided pyridinium **4e** represents the first example of organocatalyzed aldol process that exploits pyruvic acid as a pronucleophile.[11] The relative configuration of the C7 and C8 stereocenters in pyridinium salts **4a**–**4h** was assumed based on the configurations in compounds **4a** and **4e** that were obtained by X-ray diffraction studies (Scheme 2 and Scheme 3). However, it is worthy of note that, in the solid state, a *cis*-C7–C9 relative configuration is found in compound **4a**, whilst it is *trans* in compound **4e** (see below).

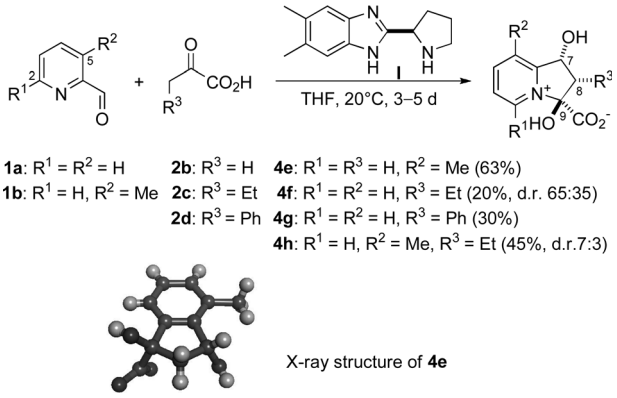

Scheme 3. Access to pyridinium salts **4e**–**4h** from pyruvic-acid derivatives **2b**–**2d** and the X-ray structure of pyridinium salt **4e**.

Then, the pyridinium ring was fully hydrogenated as above, under PtO_2 catalysis,[9] thereby affording the corresponding indolizidines **5a**–**5d** (Scheme 4). Esterification of the products with $TMSCHN_2$ furnished their corresponding methyl esters in good yields, but their enantiomeric excesses could not be measured by chiral HPLC. Better results were obtained by performing the direct benzylation of compounds **5a**–**5d** after hydrogenation of compounds **4a**–**4c**

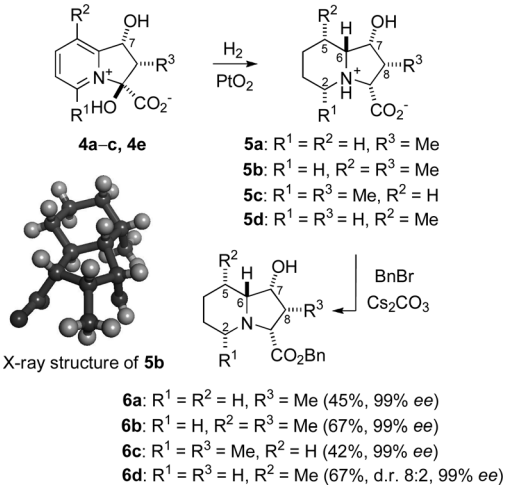

Scheme 4. Access to indolizidines **6a**–**6d** from pyridinium salts **4** and the X-ray structure of pyridinium salt **5b**.

and **4e**, thus affording UV-active benzyl esters **6a–6d** in good yields (Scheme 4). Enantiomeric excesses, as measured by chiral HPLC, showed that compounds **6a–6d** were essentially pure. The relative configuration of acid **5b**, which was obtained through the catalytic reduction of compound **4b**, was determined by X-ray diffraction analysis, which allowed us to assign similar configurations for benzyl esters **6a–6d**.

Crystallographic studies on compounds **4a** and **4e** (confirmed by X-ray analysis of compounds **5a** and **5b**) showed that the secondary alcohol at the C7 position in pyridinium salts **4a–4h** possessed an *R* configuration, in good agreement with that in isotetronic acids that were previously prepared through BIP-**I**-catalyzed aldol reaction between a variety of aldehydes and α-ketoacids.[4] Consequently, we can assume that isotetronic acids **3e–3k** bear a similar *R* configuration. The aldol process provides a second stereogenic center at the C8 position (e.g., intermediate **B**), which, according to transition state **A**, should possess an *S* configuration (Scheme 5). This stereochemistry is lost through enolization during the subsequent lactonization step into isotetronic acids **3e–3k**, but it is retained upon the formation of pyridinium salts **4**. Based on transition state model **A**,[4,12] we can conclude that the cyclization of aldol adduct **B** into pyridinium salts **4a–4h** occurs with retention of the configuration at the C8 position. Finally, the relative configuration of the stereocenters at the C2/C5 and C6 positions on the six-membered ring in compounds **6a–6d** is fully consistent with the PtO_2-catalyzed hydrogenation step occurring from the top face (e.g., model **C**), that is, *anti* to the OH and R^3 substituents on the five-membered ring. Similarly, the stereochemistry at the C9 position is fixed during the hydrogenation from the same face of an iminium intermediate.

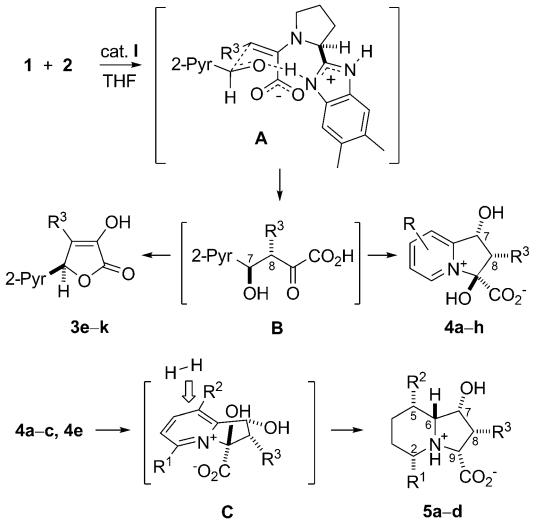

Scheme 5. Transition-state models for the aldol and hydrogenation processes.

Disappointingly, efforts to partially reduce the pyridinium ring in compounds **4** by using borohydrides ($NaBH_3CN$),[13] dithionite,[14] or Hantzsch esters[15] failed, whilst hydrogenation by using $[Ir(cod)_2Cl_2]/H_2$ (cod = 1,5-cyclooctadiene)[16] led to complete hydrogenation. Most interestingly, the treatment of pyridinium salts **4a**,**b** with H_2O_2 in MeOH led to esters **7a**,**b** in excellent yields after conversion of their corresponding acids with $TMSCHN_2$ (Scheme 6).[17] The formation of compounds **7a**,**b** through oxidative decarboxylation likely involves the oxidation of the carboxylic acid into a peracid, followed by a Baeyer–Villiger-type process.[18] Tentative allylation of the pyridinium salts in the presence of allylindium[19] in water did not give the expected allyldihydropyridine, but rather afforded the highly substituted butyrolactones (**8a**,**b**), which resulted from nucleophilic addition onto the α-keto group, with good diastereocontrol and high enantioselectivity, albeit in modest yields.[20] Finally, the enantiomeric excesses of compounds **7a**,**b** and **8a**,**b** confirmed the high enantiopurity of pyridinium salts **4a**,**b**, as estimated above.

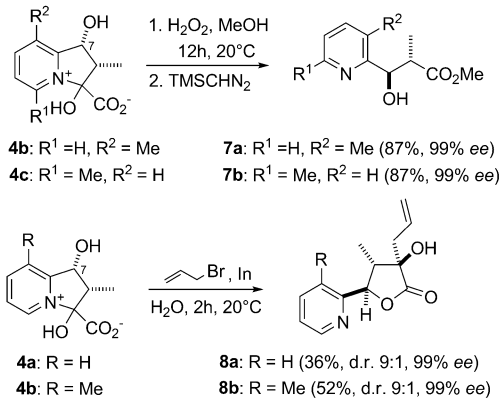

Scheme 6. Further transformations of pyridinium salts **4a–4c**.

At this point, several questions remained unanswered, that is, 1) the difference in reactivity between pyridine carbaldehydes **1a–1d** and **1e–1k**; 2) the behavior of pyridinium salts **4c** and **4d**, which were prone to afford isotetronic acids after standing for a short period of time in solution (whereas compound **4b** was indefinitely stable for at least one year!); and 3) the observation that compound **4a** crystallized as its 7-OH/9-OH *cis* isomer, whereas pyridinium **4e** crystallized as its 7-OH/9-OH *trans* isomer (Scheme 2 and Scheme 3).[21] To answer these questions and to gain a better insight into the mechanism of pyridinium formation and the nature of the equilibria that are involved in the process, DFT computational studies were performed (see the Experimental Section and the Supporting Information). Starting from ketoacid **9**, which was formed from the organocatalyzed aldolization reaction, two different pathways were envisaged. The pyridine nitrogen center could attack the ketone group, thereby affording the pyridinium salts (**4**) as *cis* or *trans* isomers, depending on which diastereotopic face of the ketone was attacked. Alternatively, the alcohol function could react with the carboxylic acid group, thereby affording compound

10 and, finally, the isotetronic acid **3**, after dehydration and keto/enol isomerization (Scheme 7).

Computation of the energies of all of the species, as well as the transition states, in the reaction of pyridine-2-carbaldehyde **1a** led to the following results. Whereas in the gas phase, pyridinium salts were much higher in energy than isotetronic acids, calculations in THF (the optimal solvent experimentally) by using IEFPCM as the continuum solvation model revealed that pyridinium *trans* isomer $\mathbf{4a}_{trans}$ was almost isoenergetic with the isotetronic acid and should be the compound present in solution (Figure 1).[22] The energy of the transition state between compound **9** and the pyridinium salts was very low (3–7 kcal mol^{-1}); thus, the equilibrium should be very fast. In contrast, the much-higher calculated energy barrier ($\mathbf{TS}_{tet}$) for the conversion of the free acid **9** into intermediate **10** was in good agreement with the sole formation of the pyridinium salt from this aldehyde.

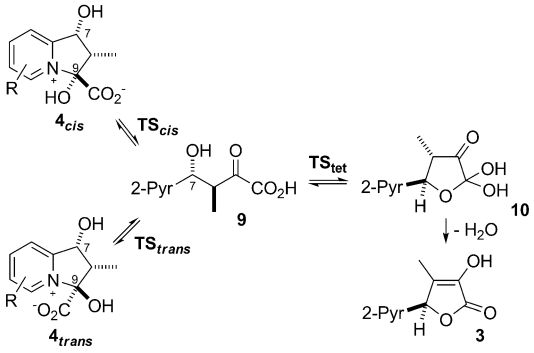

Scheme 7. Equilibria and species that are involved in the reaction.

The energies of the 2-pyridinium salts, the free acid, and the isotetronic acid were computed for eight different aldehydes, four of which led to the pyridinium salts (**1a**–**1d**), whilst the other four afforded isotetronic acids (**1e**, **1h**, **1j**, and **1k**). A clear picture emerges when comparing the three particular cases shown in Figure 2. For aldehyde **1b**, the exclusive formation of the pyridinium salt $\mathbf{4b}_{trans}$ may be explained by its greater stability compared to that of its isotetronic form (−2.8 kcal mol^{-1}). In contrast, the computed energies of pyridinium salt $\mathbf{4d}_{trans}$, which was obtained from aldehyde **1d**, revealed that isomer $\mathbf{4d}_{trans}$ was the kinetic product, thus explaining its strong tendency to isomerize into the thermodynamically more stable isotetronic **3d** upon standing in solution. Finally, with aldehyde **1e**, the free acid form **9** was more stable than the 2-pyridinium salt **4** (8.3 versus 6.1 kcal mol^{-1}); thus, the compound has no option other than forming the isotetronic acid **3e**.

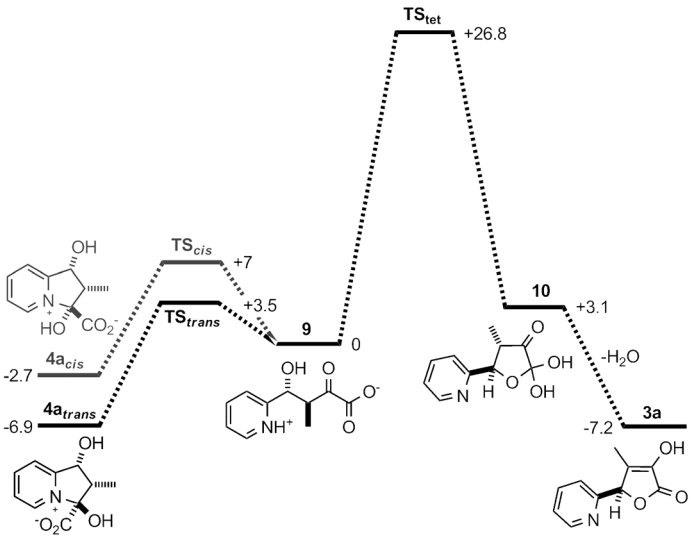

Figure 1. Energy profile [kcal mol^{-1}] of the reaction pathway at the M06-2X/6-31+G(d,p) level of theory in THF for aldehyde **1a**.

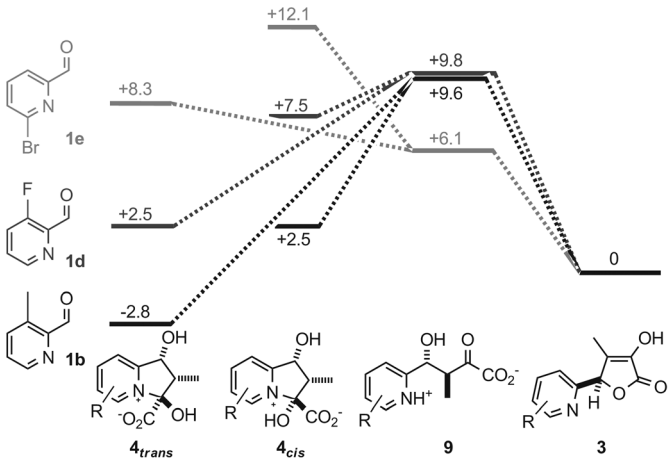

Figure 2. Comparison of the energy profiles [kcal mol^{-1}] at the M06-2X/6-31+G(d,p) level of theory in THF for aldehydes **1b**, **1d**, and **1e**.

When comparing the values of eight aldehydes (Table 3), the difference between the two sets of aldehydes is clear and is in good agreement with the experimental observations. Although the isotetronic acids are always the more-stable compounds (except for compound **1b**, for which pyridinium salt **4b** is more stable), a clear difference can be seen in terms of the energy difference between the isotetronic acids and the pyridinium salts ($\Delta G_{4trans-3}$). The energy difference between the aldehydes that afford pyridinium

Table 3. Differences in Gibbs free energy (in kcal mol^{-1}) between the species that were involved in the reactions of eight different aldehydes.

1	ΔG_{3-9}	$\Delta G_{4trans-9}$	ΔG_{4cis-9}	$\Delta G_{4trans-3}$
1a	−7.2	−6.9	−2.7	0.3
1b	−9.6	−12.4	−7.1	−2.8
1c	−7.4	−5.5	−1.1	1.9
1d	−9.8	−7.3	−2.3	2.5
1e	−6.1	2.2	5.9	8.3
1h	−7	−3.1	1.9	3.9
1j	−6.8	−3.3	1.0	3.5
1k	−7.2	−1.1	2.8	6.1

salts is small, whilst it is much larger between those that afford isotetronic acids, thus confirming the experimentally observed difference in reactivity. The energy difference between the free acids **9** and the isotetronic acids **3** (ΔG_{3-9}) were within the same range for all of the aldehydes that were considered; the difference in reactivity was due to stabilization/destabilization of the pyridinium forms by the pyridine substituents. The destabilization of the pyridinium salts was striking in terms of the energy difference between the free acid and the *cis*/*trans* pyridinium (ΔG_{4cis-9}, $\Delta G_{4trans-9}$), for which marked differences between the eight aldehydes were observed.

Thus, the calculations and experimental results strongly suggest that the pyridinium salt that is present in solution is the *trans* isomer. Interestingly, single-crystal X-ray diffraction established a *cis*-C7–C9 relative configuration in compound **4a**. To determine which form was present in solution, IR and VCD studies were performed to determine the relative and absolute configurations of compound **4b** in solution. These spectroscopic methods, in combination with DFT calculations, are well-established methods for the determination of the absolute configuration and solution conformation of chiral molecules.[23] Thus, a comparison of the experimental IR and VCD spectra with the calculated spectra for isomers $\mathbf{4b}_{trans}$ and $\mathbf{4b}_{cis}$ should allow us to assess which diastereoisomer is predominant in solution.

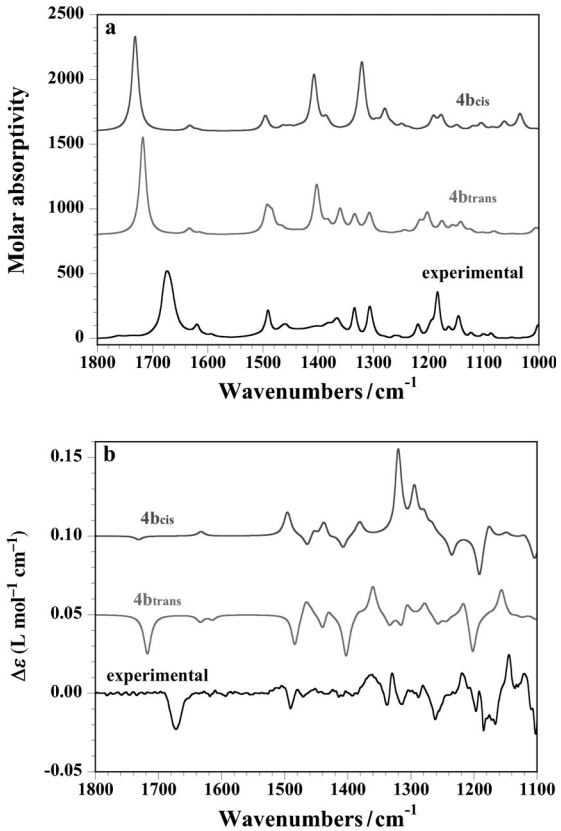

Figure 3. Comparison of the experimental a) IR and b) VCD spectra in CD_3CN with those calculated at the CAM-B3LYP/aug-cc-pVTZ DFT level of theory for diastereomers $\mathbf{4b}_{trans}$ and $\mathbf{4b}_{cis}$.

IR and VCD spectra of pyridinium **4b** were recorded in CD_3CN and are shown in Figure 3a, b, respectively. Calculated IR and VCD spectra of isomers $\mathbf{4b}_{trans}$ and $\mathbf{4b}_{cis}$ at the CAM-B3LYP/aug-cc-pVTZ level of theory are also shown in Figure 3a, b, respectively. It is clear that the experimental IR spectrum is well reproduced by the one calculated for the $\mathbf{4b}_{trans}$ isomer, whereas strong divergences are observed for the $\mathbf{4b}_{cis}$ isomer. It is noteworthy that a frequency shift is observed for the stretching *n*C=O vibrations of the carboxylate groups due to intermolecular interaction with the solvent and that the intense band calculated at 1403 cm^{-1} for the C-O-H bending appears as a very broad band with weak intensity in the experimental spectrum. The VCD spectrum confirmed the presence of the *trans* isomer in CD_3CN solution, because the calculated bands for the $\mathbf{4b}_{trans}$ isomer correlated and agreed in sign for most of the vibrational modes that were observed in the experimental spectrum. Finally, the IR and VCD spectra were recorded in CD_3OD, because this solvent was used to crystallize compound **4a**. DFT calculations were performed on the deuterated hydroxyl form of pyridinium **4b** to take into account the H/D exchange. Once again, good agreement was obtained between the experimental IR and VCD spectra and those calculated for the $\mathbf{4b}_{trans}$ isomer (see the Supporting Information), thus revealing its presence in CD_3OD solution. Thus, theoretical analysis of the reaction is valid and the isolation of the *cis* isomer by recrystallization is most likely due to a shift in the equilibrium during the crystallization process.

Conclusion

In summary, asymmetric aldol reactions between pyridine carbaldehydes and α-keto acids catalyzed by benzimidazole pyrrolidine **I** lead to aldol adducts that cyclized through two different pathways, depending on the substitution pattern of the pyridine nucleus, thereby affording either pyridinium salts or isotetronic acids. Further functionalization of the pyridinium salts **4** was shown to provide access to valuable building blocks in their enantiomerically pure form, including indolizidines, aldol products, and butyrolactones. Rationalization of both pathways was provided through DFT studies, which correlated well with experimental observations. For example, the formation of pyridinium salt **4b** as a unique compound was explained by its greater stability compared to that of its isotetronic form. In contrast, other less-stable pyridinium salts, such as compounds **4c** and **4d**, tended to rearrange into their corresponding isotetronic acids, a feature that was also well-illustrated by the DFT calculations.

Experimental Section

Preparation of compound 4a: To a solution of 2-ketobutyric acid (**2a**, 441 mg, 4.3 mmol, 1 equiv) in THF (13 mL) were added 2-pyridine carboxaldehyde (**1a**, 409 mg, 4.3 mmol, 1 equiv) and catalyst **I** (10 mol%). The reaction mixture was stirred at RT for 3 days under a N_2 atmosphere. Filtration of the precipitate afforded the desired compound (**4a**) as a white solid (661 mg, 73% yield). Single crystals suitable for X-ray diffraction analysis were grown by the slow diffusion of Et_2O into a solution of compound **4a** in MeOH. $R_f = 0.23$ (CH_2Cl_2/MeOH, 97:3); $[\alpha]_D^{25} = -34.3$ ($c = 0.56$, MeOH); m.p. 138 °C; ^{1}H NMR (300 MHz, CD_3OD): $\delta = 8.83$ (d, $J = 6.0$ Hz, 1H), 8.58 (dt, $J = 0.9$, 7.8 Hz, 1H), 8.17 (d, $J = 7.8$ Hz, 1H), 8.04 (t, $J = 6.6$ Hz, 1H), 5.47 (br s, 1H), 2.99 (br s, 1H), 1.15 ppm (d, $J = 6.0$ Hz, 3H); ^{13}C NMR (50 MHz, CD_3OD): $\delta = 170.4$ (Cq), 158.7 (Cq_{Ar}), 147.9 (CH_{Ar}), 137.8 (CH_{Ar}), 128.6 (CH_{Ar}), 125.9 (CH_{Ar}), 104.2 (Cq), 73.5 (CH), 46.6 (CH), 7.9 ppm (CH_3); IR (ATR): $\tilde{\nu} = 3255$, 2754, 1631, 1213, 1038 cm^{-1}; HRMS (ESI): m/z calcd for $C_{10}H_{11}NO_4Na$: 232.0580 $[M+Na]^+$; found: 232.0585.

Preparation of compound 3e: To a solution of 2-ketobutyric acid (**2a**, 103 mg, 1 mmol, 1 equiv) in CH_2Cl_2 (3 mL) were added 6-Bromo-2-pyridine carboxaldehyde (**1e**, 103 mg, 1 mmol, 1 equiv) and catalyst **I** (10 mol%). The reaction mixture was stirred at RT for 3 days under a N_2 atmosphere. After concentration in vacuo, purification by column chromatography on silica gel (CH_2Cl_2/MeOH, 98:2) afforded the desired compound (**3e**) as a yellow oil (239 mg, 89% yield). $R_f = 0.2$ (CH_2Cl_2/MeOH, 98:2); $[\alpha]_D^{25} = +161$ ($c = 0.84$, MeOH); ^{1}H NMR (300 MHz, CD_3OD): $\delta =$ 7.74 (dd, $J = 7.8$, 7.5 Hz, 1H), 7.59 (dd, $J = 0.6$, 7.8 Hz, 1H), 7.36 (dd, $J =$ 0.6, 7.8 Hz, 1H), 5.73 (br d, $J = 1.5$ Hz, 1H), 1.78 ppm (d, $J = 1.2$ Hz, 3H); ^{13}C NMR (150 MHz, CD_3OD): $\delta = 171.4$ (Cq), 158.2 (Cq_{Ar}), 142.8 (Cq_{Ar}), 141.4 (CH_{Ar}), 139.6 (Cq), 131.4 (Cq), 129.6 (CH_{Ar}), 121.6 (CH_{Ar}), 83.0 (CH), 9.5 ppm (CH_3); IR (ATR): $\tilde{\nu} = 1749$, 1695, 1206 cm^{-1}; HRMS (ESI): m/z calcd for $C_{10}H_8BrNO_3Na$: 291.95852 $[M+Na]^+$; found: 291.9586; HPLC (Chiralpak IA column; n-hexane/iPrOH, 90:10; flow rate: 1.0 mL min^{-1}; $\lambda = 265$ nm): $t = 11.1$ (*ent*-1), $t = 12.1$ min (*ent*-2).

Preparation of compound 6a: To a solution of pyridinium **4a** (66.5 mg, 0.32 mmol, 1 equiv) in MeOH (1 mL) was added PtO_2 (5 mol%) and the reaction mixture was pressurized with H_2 gas (balloon). The reaction mixture was stirred at RT for 24 h. After filtration over celite and concentration in vacuo, the crude residue was dissolved in DMF (0.5 mL). Cesium carbonate (0.22 mmol, 1.1 equiv) and benzyl bromide (0.20 mmol, 1 equiv) were added and the reaction mixture was stirred overnight. The product was extracted with Et_2O and the organic layer washed with water (3×25 mL) and dried over sodium sulfate. Concentration in vacuo, followed by purification by column chromatography on silica gel (CH_2Cl_2/MeOH, 99:1), afforded compound **6a** as a yellow oil (35 mg, 45% yield). $R_f = 0.25$ (CH_2Cl_2/MeOH, 98:2); $[\alpha]_D^{25} = +38$ ($c = 0.95$, MeOH); ^{1}H NMR (300 MHz, $CDCl_3$): $\delta = 7.44$–7.23 (m, 5H), 5.15 (ABq, $J = 12.3$ Hz, 2H), 3.67 (dt, $J = 3.0$ Hz, 1H), 3.26 (d, $J = 10.5$ Hz, 1H), 2.94 (br d, $J = 10.5$ Hz, 1H), 2.52–2.11 (m, 4H), 1.91–1.44 (m, 5H), 1.31–1.07 (m, 1H), 0.95 ppm (d, $J = 7.5$ Hz, 3H); ^{13}C NMR (75 MHz, $CDCl_3$): $\delta =$ 172.5 (Cq), 134.7 (Cq_{Ar}), 127.6 (CH_{Ar}), 127.4 (CH_{Ar}), 127.3 (CH_{Ar}), 74.3 (CH), 67.7 (CH), 66.2 (CH), 65.5 (CH_2), 50.7 (CH_2), 38.6 (CH), 24.6 (CH_2), 24.5 (CH_2), 22.7 (CH_2), 9.3 ppm (CH_3); IR (ATR): $\tilde{\nu} = 3480$, 2937, 1733 cm^{-1}; HRMS (ESI): m/z calcd for $C_{17}H_{23}NO_3Na$ $[M+Na]^+$ 290.17562; found: 290.1757; HPLC (Chiralpak IA column; heptane/EtOH, 95:5; flow rate: 1.0 mL min^{-1}; $\lambda = 210$ nm): $t = 9.97$ min.

Preparation of compound 8b: To a solution of compound **4b** (75 mg, 0.34 mmol, 1 equiv) in water (3.3 mL) were added allyl bromide (47 μL, 0.5 mmol, 1.5 equiv) and indium (58 mg, 0.5 mmol, 1.5 equiv). The reaction mixture was stirred at RT for 4 h. Then, the milky white reaction mixture was concentrated in vacuo. Extraction with CH_2Cl_2 and washing of the organic layer with a saturated aqueous solution of NH_4Cl, followed by purification by column chromatography on silica gel (CH_2Cl_2/MeOH, 99:1) afforded the desired compound (**8b**) as a colorless oil (32.4 mg, 24% yield, d.r. 9:1). $R_f = 0.2$ (CH_2Cl_2/MeOH, 98:2); ^{1}H NMR (600 MHz, $CDCl_3$): $\delta = 8.43$ (dd, $J = 1.2$, 4.8 Hz, 1H), 7.70 (ddd, $J = 0.4$, 1.2, 8 Hz, 1H), 7.31 (dd, $J = 4.8$, 7.6 Hz, 1H), 6.07–5.95 (m, 0.1H; diastereomer 2 (d2)), 5.94–5.82 (m, 0.9H; diastereomer 1 (d1)), 5.50 (d, $J = 9.6$ Hz, 0.9H; d1), 5.39 (d, $J = 9.6$ Hz, 0.1H; d2), 5.28–5.11 (m, 2H), 3.08 (dq, $J = 7.0$, 9.7 Hz, 0.1H; d2), 2.85 (dq, $J = 6.8$, 9.7 Hz, 0.9H; d1), 2.64 (ddt, $J = 1.2$, 6.9, 14.0 Hz, 1H), 2.57 (ddt, $J = 1.07$, 7.8, 14.0 Hz, 1H), 2.45 (s, 0.3H; d2), 2.44 (s, 2.7H; d1), 1.11 (d, $J = 7.2$ Hz, 0.3H; d2), 1.01 ppm (d, $J = 6.8$ Hz, 2.7H; d1); ^{13}C NMR (100 MHz, CD_3OD): $\delta = 178.8$ (Cq), 154.1 (Cq), 148.03 (Cq; d1), 147.97 (Cq; d2), 140.6 (CH; d2), 140.5 (CH; d1), 135.0 (Cq), 133.5 (CH; d1), 133.5 (CH; d2), 125.3 (CH; d2), 125.2 (CH; d1), 119.7 (CH_2), 82.7 (CH; d1), 81.4 (CH; d2), 77.2 (C9), 47.3 (CH; d2), 44.0 (CH; d1), 40.5 (CH_2; d1), 38.5 (CH_2; d2), 18.3 (CH_3; d1), 18.2 (CH_3; d2), 9.7 (CH_3; d2), 8.4 ppm (CH_3; d1); IR (ATR): $\tilde{\nu} = 3441$, 2981, 2950, 1734 cm^{-1}; HPLC (Chiralpak IA column; CH_2Cl_2/n-hexane/EtOH, 70:29:1; flow rate: 1.0 mL min^{-1}; $\lambda = 265$ nm): $t = 5.3$ (minor diastereomer), 10.0 min (major diastereomer); HRMS (ESI): m/z calcd for $C_{14}H_{17}NO_3$: 270.11061 $[M+Na]^+$; found: 270.1102.

X-ray crystallography data: CCDC-943762 (**4a**), CCDC-943765 (**4e**), CCDC-943763 (**5a**), and CCDC-943764 (**5b**) contain the supplementary crystallographic data for this paper. These data can be obtained free of charge from The Cambridge Crystallographic Data Centre via www.ccdc.cam.ac.uk/data_request/cif.

IR and VCD measurements: IR and VCD spectra were recorded on a ThermoNicolet Nexus 670 FTIR spectrometer that was equipped with a VCD optical bench.[24] The light beam was focused onto the sample by using a BaF_2 lens (focal length: 191 mm), passed through an optical filter (which depended on the spectroscopic range to be studied), a BaF_2 wire-grid polarizer (Specac), and a ZnSe photoelastic modulator (Hinds Instruments, Type II/ZS50). Then, the light was focused by using a ZnSe lens (focal length: 38.1 mm) onto a HgCdTe detector (1×1 mm^2, ThermoNicolet, MCTA* E6032). IR and VCD spectra were recorded at a resolution of 4 cm^{-1}, by co-adding 50 scans and 24000 scans (acquisition time: 8 h), respectively. The sample was held in a fixed-path-length cell (100 μm) with BaF_2 windows. IR and VCD spectra of compound **4b** were recorded in CD_3CN and CD_3OD at a concentration of 75 mM. Baseline corrections of the VCD spectra were performed by subtracting the bare VCD spectra of the solvents. In all experiments, the photoelastic modulator was adjusted for maximum efficiency at 1400 cm^{-1}. Calculations were performed by using the standard ThermoNicolet software, with Happ and Genzel apodization, de-Haseth phase-correction, and a zero-filling factor of one. Calibration spectra were recorded by using a birefringent plate (CdSe) and a second BaF_2 wire-grid polarizer, according to a literature procedure.[25] Finally, the solvent absorption was subtracted in the presented IR spectra.

Computational details: The geometry optimizations, vibrational frequencies, absorptions, and VCD intensities were calculated by using the Gaussian 09 program[26] at the Computer Center "Pôle Modélisation" of the Institut des Sciences Moléculaires (University Bordeaux I). To determine the energy profiles of the reactions, the M06–2X exchange-correlation functional[27] was used with a standard double-ζ 6–31+G(d,p) basis set. A polarizable continuum model (IEFPCM), as implemented in Gaussian 09, was used to describe the medium (MeOH, THF, MeCN). All of the structures were optimized and frequency calculations were performed to ensure that there were no imaginary frequencies in the local minima and only one imaginary frequency in the transition states. The connectivity between the stationary points was established by intrinsic reaction coordinate (IRC) calculations. Additional calculations of the optimized geometries of diastereomers $\mathbf{4b}_{cis}$ and $\mathbf{4b}_{trans}$ were performed by using density functional theory level with the CAM-B3LYP functional[28] and the aug-cc-pVTZ basis set. Vibrational frequencies and IR and VCD intensities were calculated at the same level of theory for the isolated molecule in vacuo, by utilizing the magnetic-field-perturbation method with gauge-invariant atomic orbitals.[29] Calculations were performed with OH and OD hydroxyl groups for comparison with the IR and VCD spectra in CD_3CN and CD_3OD, respectively. For comparison to the experimental data, the calculated frequencies were scaled by a factor of 0.965 and the calculated intensities were converted into Lorentzian bands with a half-width of 7 cm^{-1}.

Acknowledgements

We thank the CNRS and the MENRT for financial support. We gratefully acknowledge Dr. Laurent Chabaud (ICSN, Gif s/Yvette) and Antoine Jacquet (ISM, u-Bordeaux) for performing the chiral HPLC measurements and Dr. Brice Kaufmann (IECB, u-Bordeaux) for performing the X-ray diffraction studies.

[1] a) For a historical perspective on aminocatalysis, see: B. List, *Angew. Chem.* **2010**, *122*, 1774; *Angew. Chem. Int. Ed.* **2010**, *49*, 1730; b) B. List, R. A. Lerner, C. F. Barbas III, *J. Am. Chem. Soc.* **2000**, *122*, 2395.

[2] a) G. Guillena in *Modern Methods in Stereoselective Aldol Reactions* (Ed.: R. Mahrwald), Wiley-VCH, Weinheim, **2013**, Chapter 3, pp. 155–268, and references therein; b) L. M. Geary, P. G. Hultin, *Tetrahedron: Asymmetry* **2009**, *20*, 131; c) B. M. Trost, C. S. Brindle, *Chem. Soc. Rev.* **2010**, *39*, 1600; d) G. Guillena, D. J. Ramon, C. Najera in *Enantioselective Organocatalyzed Reactions II* (Ed.: R. Mahrwald), Springer, Dordrecht, **2011**, pp. 245–342; e) X.-W. Wang, Y. Wang, J. Jia in *Science of Synthesis, Vol. 1* (Eds.: B. List, K. Maruoka), Georg Thieme Verlag, Stuttgart, **2011**, pp. 1–34; f) S. M. Yliniemelä-Sipari, A. Piisola, P. M. Pihko in *Science of Synthesis, Vol. 1* (Eds.: B. List, K. Maruoka), Georg Thieme Verlag, Stuttgart, **2011**, pp. 35–72.

[3] a) E. Lacoste, E. Vaique, M. Berlande, I. Pianet, J.-M. Vincent, Y. Landais, *Eur. J. Org. Chem.* **2007**, 167; b) E. Lacoste, Y. Landais, K. Schenk, J.-B. Verlhac, J.-M. Vincent, *Tetrahedron Lett.* **2004**, *45*, 8035.

[4] J.-M. Vincent, C. Margottin, M. Berlande, D. Cavagnat, T. Buffeteau, Y. Landais, *Chem. Commun.* **2007**, 4782.

[5] a) J. Bigorra, J. Font, O. C. de Echaguen, R. M. Ortuno, *Tetrahedron* **1993**, *49*, 6717; b) D. Enders, H. Dyker, F. R. Leusink, *Chem. Eur. J.* **1998**, *4*, 311; c) N. Gathergood, K. Juhl, T. B. Poulsen, K. Thordrup, K. A. Jorgensen, *Org. Biomol. Chem.* **2004**, *2*, 1077; d) P. Dambruoso, A. Massi, A. Dondoni, *Org. Lett.* **2005**, *7*, 4657; e) W. Raimondi, D. Bonne, J. Rodriguez, *Angew. Chem.* **2012**, *124*, 40; *Angew. Chem. Int. Ed.* **2012**, *51*, 40; f) W. Raimondi, D. Bonne, J. Rodriguez, *Chem. Commun.* **2012**, *48*, 6763.

[6] a) T. Namiki, M. Nishikawa, Y. Itoh, I. Uchida, M. Hashimoto, *J. Antibiot.* **1987**, *40*, 1400; b) M. Suzuki, Y. Hosaka, H. Matsushima, T. Goto, T. Kitamura, K. Kawabe, *Cancer Lett.* **1999**, *138*, 121; c) A. J. Pallenberg, J. D. White, *Tetrahedron Lett.* **1986**, *27*, 5591; d) G. Stork, S. D. Rychnovsky, *J. Am. Chem. Soc.* **1987**, *109*, 1564.

[7] B. Zhang, Z. Jiang, X. Zhou, S. Lu, J. Li, Y. Liu, C. Li, *Angew. Chem. Int. Ed.* **2012**, *51*, 13159.

[8] For selected recent syntheses of indolizidines, see: a) G. Lapointe, K. Schenk, P. Renaud, *Chem. Eur. J.* **2011**, *17*, 3207; b) S. V. Pronin, G. Tabor, D. J. Jansen, R. A. Shenvi, *J. Am. Chem. Soc.* **2012**, *134*, 2012; c) X.-G. Hu, B. Bartholomew, R. J. Nash, F. X. Wilson, G. W. J. Fleet, S. Nakagawa, A. Kato, Y.-M. Jia, R. van Well, C.-Y. Yu, *Org. Lett.* **2010**, *12*, 2562.

[9] D. Giomi, R. Alfini, A. Micoli, E. Calamai, C. Faggi, A. Brandi, *J. Org. Chem.* **2011**, *76*, 9536.

[10] Compounds **4f** and **4h** were obtained as a mixture of two diastereomers at the C9 position.

[11] M. J. Walters, E. J. Toone, *Nat. Nanotechnol. Nat. Protocols* **2007**, *2*, 1825.

[12] S. Bahmanyar, K. N. Houk, *J. Am. Chem. Soc.* **2001**, *123*, 12911.

[13] M. Mehmandoust, C. Marazano, R. Singh, B. Gillet, M. Cesario, J. L. Fourrey, B. C. Das, *Tetrahedron Lett.* **1988**, *29*, 4423.

[14] V. Carelli, F. Liberatore, L. Scipione, B. Di Rienzo, S. Tortorella, *Tetrahedron* **2005**, *61*, 10331.

[15] A. Bruckmann, M. A. Pena, C. Bolm, *Synlett* **2008**, 900.

[16] a) J. A. Bull, J. J. Mousseau, G. Pelletier, A. B. Charrette, *Chem. Rev.* **2012**, *112*, 2642; b) C. Y. Legault, A. B. Charette, *J. Am. Chem. Soc.* **2005**, *127*, 8966.

[17] a) D. Seyferth, H. Menzel, A. W. Dow, T. C. Flood, *J. Am. Chem. Soc.* **1968**, *90*, 1080; b) D. Seyferth, H. Menzel, A. W. Dow, T. C. Flood, *J. Organomet. Chem.* **1972**, *44*, 279.

[18] a) C. W. Jefford, A. F. Boschung, A. B. M. Bolsman, R. M. Moriarty, B. Melnick, *J. Am. Chem. Soc.* **1976**, *98*, 1017; b) L. Ju, A. R. Lippert, J. W. Bode, *J. Am. Chem. Soc.* **2008**, *130*, 4253; c) A. R. Lippert, K. R. Keshari, J. Kurhanewicz, C. J. Chang, *J. Am. Chem. Soc.* **2011**, *133*, 3776.

[19] P. C. Lobben, L. A. Paquette, *J. Org. Chem.* **1998**, *63*, 6990.

[20] The conversion of compounds **4a**,**b** into compounds **8a**,**b** was complete, as shown by ^{1}H NMR spectroscopy. The moderate yields should be attributed to the high polarity and solubility of compounds **8a**,**b** in water, which resulted in the loss of material.

[21] *Cis* and *trans* isomers of pyridinium salts **4** refer to the relative configuration between the OH substituents at C7 and C9 positions. This terminology is used throughout the discussion.

[22] Additional calculations (data not shown) in MeOH and CH_2Cl_2 with the same basis set and solvation model gave similar results.

[23] a) T. B. Freedman, X. Cao, R. K. Dukor, L. A. Nafie, *Chirality* **2003**, *15*, 743; b) T. Buffeteau, L. Ducasse, A. Brizard, I. Huc, R. Oda, *J. Phys. Chem. A* **2004**, *108*, 4080; c) T. Buffeteau, D. Cavagnat, A. Bouchet, T. Brotin, *J. Phys. Chem. A* **2007**, *111*, 1045.

[24] T. Buffeteau, F. Lagugné-Labarthet, C. Sourisseau, *Appl. Spectrosc.* **2005**, *59*, 732.

[25] L. A. Nafie, D. W. Vidrine in *Fourier Transform Infrared Spectroscopy, Vol. 3* (Eds.: J. R. Ferraro, L. J. Basile), Academic Press, New York, **1982**, pp. 83–123.

[26] Gaussian 09, Revision A.02, M. J. Frisch, G. W. Trucks, H. B. Schlegel, G. E. Scuseria, M. A. Robb, J. R. Cheeseman, G. Scalmani, V. Barone, B. Mennucci, G. A. Petersson, H. Nakatsuji, M. Caricato, X. Li, H. P. Hratchian, A. F. Izmaylov, J. Bloino, G. Zheng, J. L. Sonnenberg, M. Hada, M. Ehara, K. Toyota, R. Fukuda, J. Hasegawa, M. Ishida, T. Nakajima, Y. Honda, O. Kitao, H. Nakai, T. Vreven, J. A. Montgomery, Jr., J. E. Peralta, F. Ogliaro, M. Bearpark, J. J. Heyd, E. Brothers, K. N. Kudin, V. N. Staroverov, R. Kobayashi, J. Normand, K. Raghavachari, A. Rendell, J. C. Burant, S. S. Iyengar, J. Tomasi, M. Cossi, N. Rega, J. M. Millam, M. Klene, J. E. Knox, J. B. Cross, V. Bakken, C. Adamo, J. Jaramillo, R. Gomperts, R. E. Stratmann, O. Yazyev, A. J. Austin, R. Cammi, C. Pomelli, J. W. Ochterski, R. L. Martin, K. Morokuma, V. G. Zakrzewski, G. A. Voth, P. Salvador, J. J. Dannenberg, S. Dapprich, A. D. Daniels, O. Farkas, J. B. Foresman, J. V. Ortiz, J. Cioslowski, D. J. Fox, Gaussian, Inc., Wallingford CT, **2009**.

[27] a) Y. Zhao, D. G. Truhlar, *Theor. Chem. Acc.* **2008**, *120*, 215; b) Y. Zhao, D. G. Truhlar, *Theor. Chem. Acc.* **2008**, *119*, 525; c) Y. Zhao, D. G. Truhlar, *Acc. Chem. Res.* **2008**, *41*, 157.

[28] T. Yanai, D. Tew, N. Handy, *Chem. Phys. Lett.* **2004**, *393*, 51.

[29] J. R. Cheeseman, M. J. Frisch, F. J. Delvin, P. J. Stephens, *Chem. Phys. Lett.* **1996**, *252*, 211.

Received: June 14, 2013
Published online: ■■ ▮▮, 0000

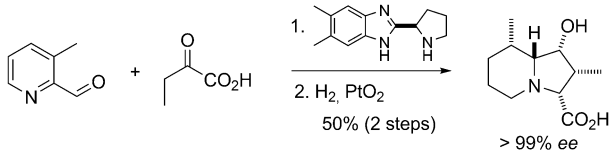

BIPpity boppity boo: Asymmetric aldol reactions between pyridine carbaldehydes and α-ketoacids were shown to provide isotetronic acids or their corresponding pyridinium salts with high enantioselectivities by using benzimidazole pyrrolidine (BIP) as a catalyst. Hydrogenation of the resulting pyridinium salts led to new indolizidines with high enantioselectivity and diasterocontrol (see scheme).

Organocatalysis

V. Liautard, D. Jardel, C. Davies, M. Berlande, T. Buffeteau, D. Cavagnat, F. Robert, J.-M. Vincent,* Y. Landais** ▮▮▮▮–▮▮▮▮

Organocatalyzed Aldol Reaction Between Pyridine-2-carbaldehydes and α-Ketoacids: A Straightforward Route towards Indolizidines and Isotetronic Acids